

Effect of Impeller Flow Path on Pump Performance and Impeller Stability of the Monopivot Circulatory Pump*

Masahiro Nishida, *Member, JSMBE*, Kento Nakayama, Ryo Kosaka, Osamu Maruyama,
Yasuo Kawaguchi, Katsuyuki Kuwana, Takashi Yamane, *Member, JSMBE*

Abstract—The effect of a cutout on the pump pressure-flow characteristics and the impeller stability was quantified using computational fluid dynamics analysis in order to provide good hemocompatibility of the monopivot extracorporeal circulation pump. As a result, the following findings were clarified. The pump pressure is lower in the cutout model than in the no-cutout model. The impeller stability with respect to the buoyancy of the impeller is better in the cutout model than in the no-cutout model. The impeller stability with respect to the impeller tilt is better in the cutout model than in the no-cutout model. Therefore, the cutout model, in which the geometry corresponds to the commercialized pump, was likely to be better than the no-cutout model because the stability that has the possibility to decrease the gap instantaneously to increase hemolysis despite the impeller rotational speed slightly.

I. INTRODUCTION

The extracorporeal circulation pump is generally used for heart failure patients during heart surgery and/or for other life support treatments during surgery. Since the monopivot extracorporeal circulation pump, the impeller of which is supported at a single contact point by a monopivot bearing, is an effective pump in which the area of the contact point between the impeller and the casing is quite small, thrombogenesis around the bearing is inhibited[1][2][3]. At present, the pump is expected to be adapted for heart surgery and operative cardiac support for several weeks.

One of the most important problems is erythrocyte rapture, which is referred to as hemolysis. Since hemolysis increases with increasing shear rate and decreasing gap width between the impeller and the casing of the pump, it is important to improve the pump pressure-flow characteristics (referred to in industry as pump performance) in order to decrease the impeller rotational speed and to maintain the impeller rotational stability to maintain the gap width so as to decrease hemolysis. In particular, since the impeller of the pump was

M. Nishida is with the National Institute of Advanced Industrial Science and Technology, Tsukuba, Japan (corresponding author to provide phone: +81-29-861-7177; fax: +81-29-861-7848; e-mail: masahiro.nishida@aist.go.jp).

K. Nakayama, is with the Department of Science and Technology, Tokyo University of Science, Noda, Japan (e-mail: nakayama-kento@aist.go.jp).

R. Kosaka is with the National Institute of Advanced Industrial Science and Technology, Tsukuba, Japan (e-mail: ryo.kosaka@aist.go.jp).

O. Maruyama is with the National Institute of Advanced Industrial Science and Technology, Tsukuba, Japan (e-mail: osamu.maruyama@aist.go.jp).

Y. Kawaguchi, is with the Department of Science and Technology, Tokyo University of Science, Noda, Japan (e-mail: yasuo@rs.noda.tus.ac.jp).

K. Kuwana, is with Senko Medical Instrument Mfg. Co. Ltd., Kasukabe, Japan (e-mail: kuwana@mera.co.jp).

T. Yamane is with the the Department of Technology, Kobe University, Kobe, Japan (e-mail: yamane@mech.kobe-u.ac.jp).

supported by a single pivot in the monopivot pump, the impeller stability in pump driving might be diminished by hydraulic force. Therefore, the cutout was adopted in the impeller in order to achieve impeller stability, where the flow path is spread over the impeller tip region. However, the effect of the cutout on the pump pressure-flow characteristics and the impeller stability has not yet been clarified from a fluid mechanical point of view.

In the present study, the effect of the cutout on the pump pressure-flow characteristics and the impeller stability was quantified using computational fluid dynamics (CFD) analysis in order to clarify the effect and obtain good hemocompatibility of the monopivot extracorporeal circulation pump.

II. METHOD

A. Objective pump

Figure 1 shows the overall geometry of the objective monopivot pump which is a commercialized extracorporeal circulation pump (MERA centrifugal pump, Senko Medical Instrument Mfg. Co., Ltd.). The impeller, the diameter of which is 50 mm, is a closed impeller having four straight flow paths that are covered by a top shroud and a bottom shroud. The impeller is supported by a monopivot bearing. The impeller rotates like a gyro as a result of motor torque through the radial magnetic coupling [3].

Figure 2 shows the impeller geometries of the cutout model and the no-cutout model which were compared in the present study. In the cutout model, which corresponds to the commercialized pump, each flow path has two cutouts on the impeller tip: a front cutout with a horizontal spreading angle of 90 ° and no vertical contracting and a rear cutout with a spreading angle of 90 ° and a vertical contracting angle of 45°, each having a depth of 4 mm, as shown in Fig. 2(a). On the other hand, in the no-cutout model, which is a virtual pump, the flow paths have no cutouts on the impeller tip, as shown in Fig. 2(a).

B. CFD analysis method

The model geometry was generated using 3D-CAD software (SolidWork, Dassault Systèmes *SolidWorks* Co.). The calculation meshes were made using commercially available software (Gridgen, Pointwise Ltd.) based on the model geometry. The number of calculation cells was approximately 1,000,000 meshes consisting of unstructured meshes. Calculations were conducted using commercially available fluid analysis solver software (STAR-CCM+ 6.02, Computational Dynamics) based on the finite volume method. The working fluid was approximated to be a Newtonian fluid having a density of 1,050 kg/m³ and the viscosity was 3 cP. Unsteady analysis was conducted using the sliding mesh

method and the standard $k-\epsilon$ model as the turbulent model. The boundary conditions were set at an inlet flow rate of 4 L/min and a pump outlet pressure of 0 mmHg, where the rated rotational speed of the impeller was 2,806 rpm. These conditions satisfy the pump pressure of 200 mmHg which is defined as a driving condition for the extracorporeal circulation use in the cutout model [3].

C. Calculations

First, in order to evaluate the pump-flow characteristics, the pump pressure P , which is the difference between the inlet pressure and the outlet pressure, was calculated as follows:

$$P = P_{outlet} - P_{inlet} \quad (1)$$

where P_{inlet} is the inlet pressure, and P_{outlet} is the outlet pressure.

Next, the hydraulic force on the impeller in the direction of the axis of rotation, F_z , was calculated in order to evaluate the impeller stability [4]. This force was calculated based on the area integral of the pressure on the impeller surface as follows:

$$F_z = \int_A \sigma_z dA \approx \int_A p_z dA \quad (2)$$

where the viscous hydraulic force was negligibly small. The negative value of F_z is defined as a buoyant force.

Furthermore, the hydraulic force moment on the impeller around the center of the pivot, M_x and M_y , were calculated in order to evaluate the impeller stability about the x and y axes, respectively, as follows:

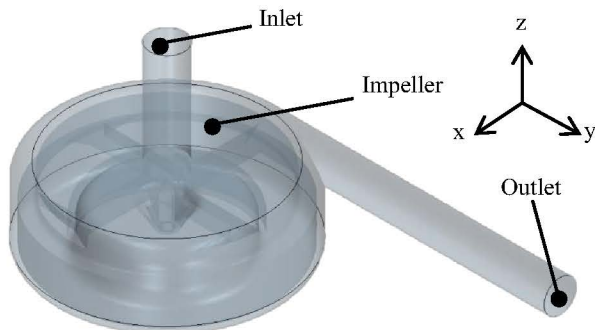
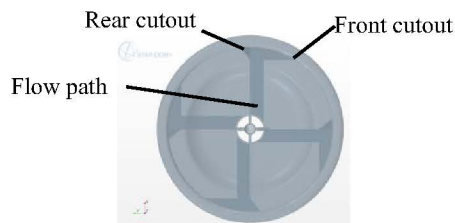
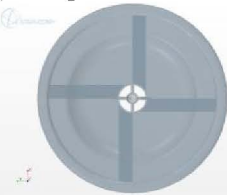


Fig. 1 Computational domain of the pump



(a) cutout model (corresponds to commercialized model)



(b) no-cutout model

Fig. 2 Geometry of the objective comparison models

$$M_x = \int_A (y\sigma_z - z\sigma_y) dA, \quad M_y = \int_A (z\sigma_x - x\sigma_z) dA \quad (3)$$

where x , y , and z are the distances from the center of the pivot bearing in the orthogonal directions, and σ_x , σ_y , and σ_z are the stresses in each of these direction [5]. The smaller the absolute values of M_x and M_y , the more stable the impeller rotates. Moreover, positive values of M_x and M_y , indicate that the impeller is tilted toward the outlet side.

III. RESULTS

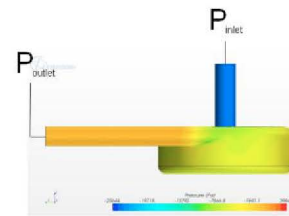
A. Pump pressure-flow characteristics

Figure 4 shows the phase variation of the pump pressure under the condition of the rated impeller rotational speed and the rated flow rate. The amplitude of the phase variation changed only slightly between the cutout model and the no-cutout model.

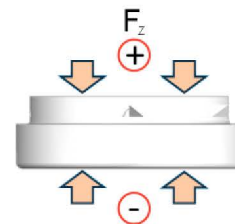
Figure 5 shows the result of average pump pressure with standard deviation during a single rotation. The pump pressure was 193 mmHg in the cutout model. Since the experimental condition resulted the pump pressure of 200 mmHg at the same rotational speed, the validation of the CFD analysis was confirmed at the error of within 4%. On the other hand, it was 211 mmHg in the no-cutout model. Therefore, the rated impeller rotational speed of the cutout model was 3 % higher than that of no-cutout model.

B. Impeller stability against the buoyant of the impeller

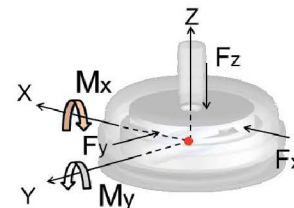
Figure 6 shows the phase variation of the hydraulic force on the impeller. The amplitude of the phase variation varied only slightly between the cutout model and the no-cutout model.



(a) pump pressure



(b) hydraulic force on the impeller



(c) hydraulic force moment on the impeller

Fig. 3 Pump pressure, hydraulic force on the impeller, and hydraulic force moment on the impeller

Figure 7 shows the results for the average hydraulic force on the impeller with standard deviation during a single rotation. The average hydraulic force on the impeller over a single rotation was 2.8 N in the cutout model and 1.7 N in the no-cutout model. Therefore, the buoyancy of the impeller in the no-cutout model was greater than that in the cutout model.

C. Impeller stability with respect to impeller tilt

Figure 8 shows the phase variation of the hydraulic force moment on the impeller about the center of the pivot. Figures 8(a) and 8(b) show the moments about the x and y axes, respectively. The amplitudes of the phase variations varied only slightly between the cutout model and the no-cutout model.

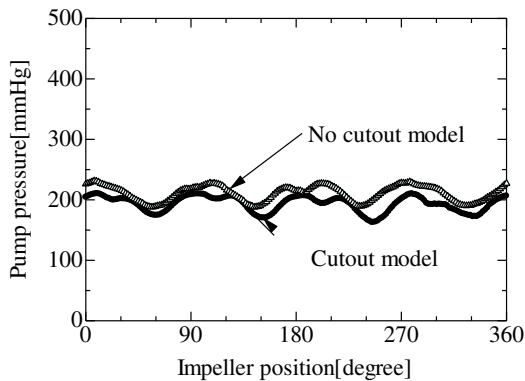


Fig. 4 Phase variation of the pump pressure

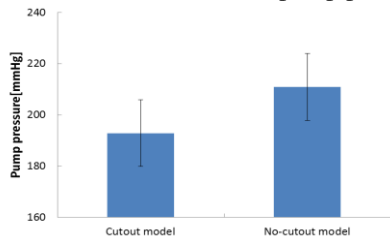


Fig. 5 Average pump pressure

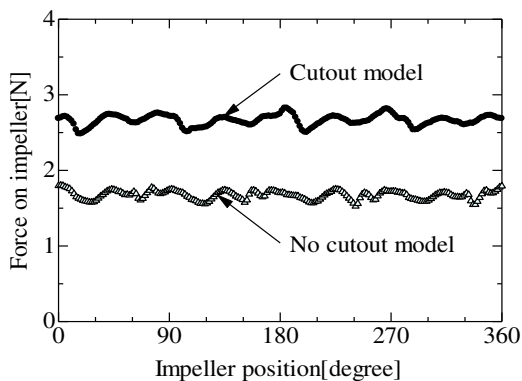


Fig. 6 Hydraulic force on the impeller

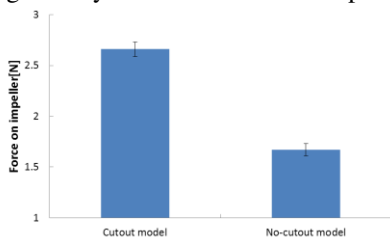


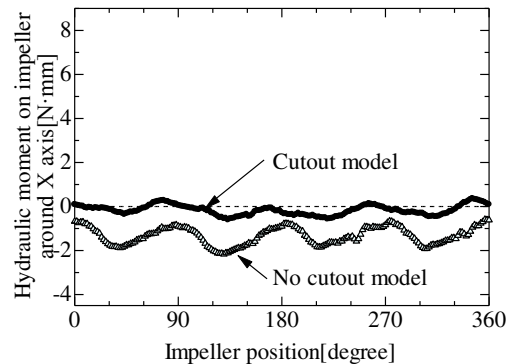
Fig. 7 Average hydraulic force on impeller

Figure 9 shows the average hydraulic force moment on the impeller about the center of the pivot with standard deviation during a single rotation. Figures 9(a) and 9(b) show the moments around the x and y axes, respectively. The average hydraulic force moment on the impeller about x axis was -0.19 N·mm in the cutout model and -1.13 N·mm in the no-cutout model. The average hydraulic force moment on the impeller about the y axis was 6.47 N·mm in the cutout model and 7.85 N·mm in the no-cutout model. Therefore, the impeller stability in the cutout model was higher than that in the no-cutout model.

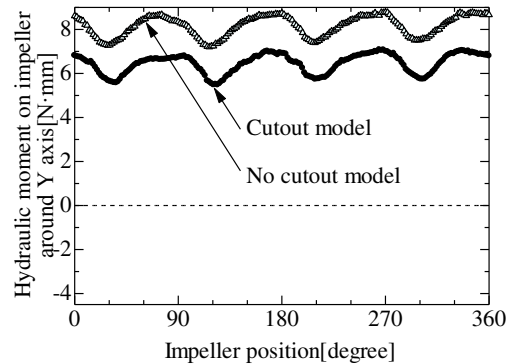
IV. DISCUSSION

A. Pump pressure-flow characteristics

The lower pump pressure in the cutout model as compared to that of the no-cutout model is related to the effective impeller diameter. The existence of the cutout decreased the impeller diameter, the “default” diameter of which was 50 mm in the no-cutout model.



(a) rotation about the X axis



(b) rotation about the Y axis

Fig. 8 Hydraulic force moment on the impeller about the center of the pivot

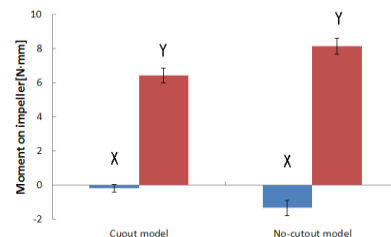


Fig. 9 Average hydraulic moment on impeller

B. Impeller stability with respect to the impeller buoyancy

The hydraulic force on the impeller depends on the pressure distribution on the impeller. Thus, the pressure contours on the surface of the cutout model and no-cutout model are shown in Figure 10. It shows that there is larger high pressure area in the volute area in the cutout model than in the no-cutout model. Fluid velocity transforms to pressure increase in the volute area. Therefore, the transformation from the fluid velocity to the pressure increase becomes more easily in the cutout model than in the no-cutout model because the effective volute area in the cutout model is larger than that in the no-cutout model. In this pump, high pressure in the volute region turns to the pushing force on the impeller toward the pump casing. So the pushing force on the impeller toward the casing is larger in the cutout model than in the no-cutout model. Therefore, the stability with respect to the buoyancy of the impeller was considered to be better in the cutout model than in the no-cutout model.

C. Impeller stability with respect to the impeller tilt

Both models generate high pressure around the impeller tip. In the cutout model, the pressure increases gradually in the radial direction because pressure increases both in the volute region and the cutout region. As such, the hydraulic force moment is easily balanced in the circumferential direction despite the existence of the outlet. This indicates that the small hydraulic force moment on the impeller stabilizes the impeller rotation with respect to impeller tilt. On the other hand, in the no-cutout model, the pressure increases dramatically in the radial direction because the pressure increases only in the volute region. Thus, the

hydraulic force moment in the circumferential direction is difficult to balance if the outlet is present. This reflects the result of the large hydraulic force moment on the impeller, which tilts the impeller rotation toward the outlet side.

In our previous pump performance study, the no-cutout model had not rotated regularly under some driving conditions while the cutout model had rotated. Thus, the cutout was used to stabilize the impeller rotation. In the pump, the minimum gap is several hundred μm between the impeller and the casing. The previous shear stress analysis suggested that the maximum shear stress attained several hundred Pa [3]. Therefore, some impeller tilt has the anxiety to increase the shear stress resulting high pump hemolysis. Moreover, in a previous flow visualization study, the cutout was found to change the flow direction around the impeller [6]. Therefore, the cutout in the impeller is important in order to smooth the flow and to circumferentially balance the pressure increase.

V. CONCLUSION

Based on computational fluid dynamics analysis of the flow in the monopivot circulatory pump, the following conclusions were obtained:

- 1) The pump pressure is lower in the cutout model than in the no-cutout model.
- 2) The impeller stability with respect to the buoyancy of the impeller is better in the cutout model than in the no-cutout model.
- 3) The impeller stability with respect to the impeller tilt is better in the cutout model than in the no-cutout model.

At present, the cutout model, the geometry of which corresponds to the commercialized pump, was likely to be better than the no-cutout model. It is because the stability is like to be more important that has the possibility to decrease the gap instantaneously to increase hemolysis. In the present study, we compared only two models. But it may be possible to improve the geometry of the flow path including cutouts in the future with considering both the pump-flow characteristics and the impeller stability with respect to the buoyancy of the impeller and the impeller tilt.

REFERENCES

- [1] T. Yamane, T. Ikeda, T. Orita, T. Tsutsui and T. Jikuya, "Design of a centrifugal blood pump with magnetic suspension", *Artificial Organs*, vol. 19, 1995, pp. 625–386.
- [2] T. Yamane, M. Nishida, T. Kijima and J. Maekawa, "New Mechanism to Reduce the Size of the Monopivot Magnetic Suspension Blood Pump : Direct Drive Mechanism", *Artificial Organs*, vol.21, 1997, pp.620–624.
- [3] M. Nishida, O. Maruyama, R. Kosaka, T. Yamane, H. Kogure, H. Kawamura, Y. Yamamoto, K. Kuwana, Y. Sankai and T. Tsutsui, "Hemocompatibility evaluation with experimental and computational fluid dynamic analyses for a monopivot Circulatory Assist Pump", *Artificial Organs*, vol. 33, 2009, pp.378–86.
- [4] A. J. Stepanoff, *Centrifugal and axial flow pumps (2nd ed)*. Florida: Krieger Publishing Company, 1993, chapters 7 & 11.
- [5] R. S. Miskovich and C. E. Brennen, "Some unsteady fluid forces on pump impellers", *Journal of Fluid Engineering*, vol. 114, 1992, pp.632–637.
- [6] H. Kogure, "Research on the hemocompatibility evaluation of a monopivot circulatory assist pump," M.S. thesis, Dept. Mech. Eng., Tokyo Univ. Sci., Chiba, Japan, 2007.

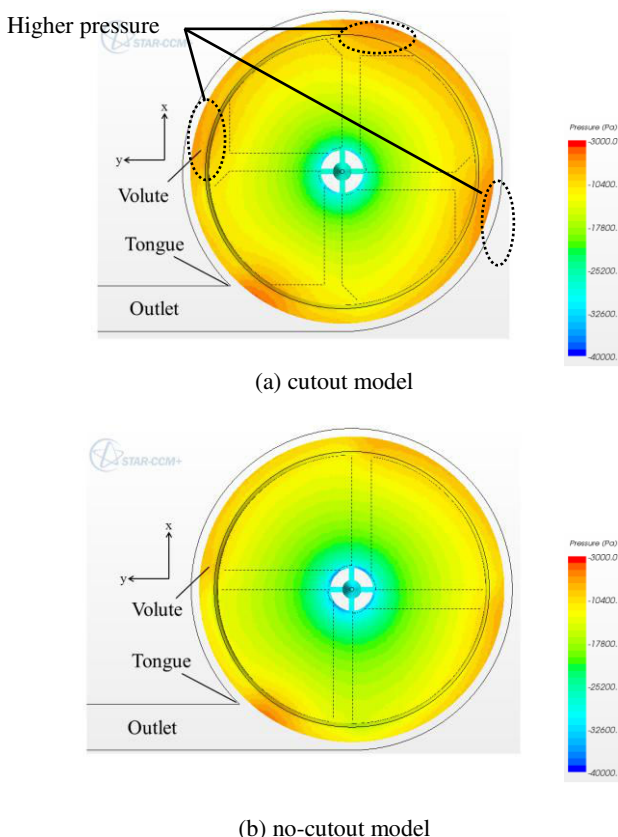


Fig. 10 Top view of pressure contour on the impeller